Potential-dependent Pt(111)/water interface: Tackling the challenge of a consistent treatment of electrochemical interfaces

Laura Braunwarth,[†,§] Christoph K. Jung,[‡,¶,§] and Timo Jacob[*,†,‡,¶]

†*Institute of Electrochemistry, Ulm University, Albert-Einstein-Allee 47, D-89081 Ulm, Germany*

‡*Helmholtz Institute Ulm (HIU) Electrochemical Energy Storage, Helmholtzstr. 11, D-89081 Ulm, Germany*

¶*Karlsruhe Institute of Technology (KIT), P.O. Box 3640, D-76021 Karlsruhe, Germany*

§*Contributed equally to this work*

E-mail: christoph.jung@kit.edu,timo.jacob@uni-ulm.de

Abstract

The interface between an electrode and an electrolyte is the location where electrochemical processes for countless technologically important applications occur. Though its high relevance and the intense efforts devoted to its elucidation, an atomic-level description of the interfacial structure and especially the dynamics of the electric double layer is still amiss. Here, we present reactive force field molecular dynamics simulations of electrified Pt(111)|water interfaces, shedding light on the orientation of water molecules in the vicinity of the Pt(111) surface, considering the influence of potential, adsorbates and ions simultaneously. We obtain a shift of the water's preferred orientation in the surface oxidation potential region, breaking with the so far proclaimed strict correlation to the free charge density. Further, the course of the entropy and the intermolecular ordering in the interfacial region complements the characterization. Our work contributes to the ongoing understanding process of electric double layers and in particular of the structure of the electrified Pt(111)|water interface and aims at providing insights into electrochemical processes occurring there.

Introduction

At the interface between an electrode and electrolyte the electric double layer (EDL), featuring a considerably large potential change within a few Ångströms and a complex interplay of charges between solvent dipoles, charged adsorbates and the diffuse ion layer, is formed. Deepened understanding of the EDL is a stringent necessity for the knowledge-based advancement of electrochemical processes occurring in technologically relevant settings such as energy conversion, storage devices and solar cells.[1–4] Despite its high significance, a complete and comprehensive atomic-level description of the EDL including interfacial structures and dynamics is so far lacking. Here, its complexity and difficulty to probe have been challenged in recent years both experimentally (*e.g.* via X-ray photoelectron spectroscopy (XPS),[1] Raman spectroscopy,[5,6] laser-induced temperature jump methods,[7] cyclic voltammetry (CV)[8] or sum frequency generation spectroscopy[9]) and theoretically via empirical interatomic force field simulations and first-principles calculations (*e.g. ab initio* molecular dynamics (AIMD),[10,11] see also ref. 12,13 and references therein).

Although theoretical approaches are attractive in providing structural information and insights into dynamic processes of electrified interfaces on an atomistic level and are able to complement experiments, several challenges still need to be tackled. Different strategies have been developed to include the electrode potential into simulations, such as the widely employed computational standard hydrogen electrode scheme,[14] having the metal electrode exchange electrons with a reservoir,[15] constant Fermi level molecular dynamics,[16,17] the electronegativity offset method,[18] by introducing fixed excess charges[10,19] or homogeneous background charges.[20] Also, the description of the aqueous electrolyte differs: From treating the solvent implicitly as a dielectric medium,[21,22] over explicit but static solvent molecules localized at the electrode[23,24] to a completely explicit modeling of the electrolyte.[10,11] Though the explicit modeling is favored in terms of polarization, solvation and accuracy the higher computational cost needs to be considered (*e.g.* limiting the number of solvent molecules in AIMD simulations to around 100). Here, force field methods can complement first princi-

ples calculations by covering significantly larger time and length scales while still providing atomistic, mechanistic and dynamic information. Already, the early conception of a frozen bilayer structure of the interfacial water on certain transition metal surfaces has been modified by including a certain degree of disorder, stressing the importance of including the water dynamics.[25–30] Furthermore, though adsorbates affect properties of the solvation layer they have not been included in the interface system of most AIMD simulations, with exceptions of selected studies considering adsorbed hydrogen[31–33] or hydroxide.[30] Adsorbates are, however, especially of interest when simulating the platinum|water interface: More detailed insights into surface coverage effects on the interfacial structure of the adsorbed water layer are highly necessary, taking into consideration the electrode being covered with oxygenated intermediates at electrode potentials relevant for catalytic reactions (*e.g.* oxygen reduction reaction).

Recently, Le *et al.* have performed state-of-the-art AIMD simulations studying the relationship between the molecular structure of the Pt(111)|water interface and its capacitive behavior.[10] Sakong *et al.* have investigated the mobility and orientation of water molecules in the adsorbate layer on the same surface, including variations of the potential.[11] Also, Bouzid *et al.* studied the structural reorganization of the electrical double layer depending on the potential with Fermi-level molecular dynamics, observing a so-called flip-flop behavior: The water molecule's dipole points towards (or away) from the Pt(111) surface when being negatively (or positively) charged.[17] However, the question is still unanswered how the interfacial water is behaving considering all relevant factors (*e.g.* potential, adsorbates and ions) simultaneously.

Motivated by these questions, in the present work we performed extensive ReaxFF reactive molecular dynamics (MD) studies of the Pt(111)|water interface under the influence of a simulated electrode potential as a function of surface charge densities and surface coverages of oxygenated intermediates. In contrast to various previous studies, we provide a fully self-consistent description of the entire electrochemical interface that includes the surface

as well as an extended part of the electrolyte region. We present a detailed analysis of the variation of interfacial water orientation with the applied potential. Our calculations demonstrate the preference of the H-down orientation, with one O−H bond directed towards the surface, in surface oxidation potential region. We further elucidate the thermodynamics of the Pt(111)|water interface by evaluating the course of the entropy from the bulk water to the adsorbed water layer. Our work highlights the importance of complementing the molecular-level picture of the potential-dependent structure and dynamics of the EDL.

Methods

ReaxFF

The ReaxFF reactive force field method is based on a bond-order-dependent potential energy term in combination with a time-dependent, polarizable charge description.[34,35] Bonding terms (*e.g.* bond, angle and torsion contributions; inherently depending on the bond order) and non-bonding interaction terms (*e.g.* van der Waals, Coulomb interactions and hydrogen bonds) contribute to the potential energy formulation. The bond order gets updated every iteration step controlled by the local atomic environment. Hereby, bond formation as well as bond dissociation can be captured. The self-consistent electron equilibration method (EEM) by Mortier *et al.*[36] is used for determining the partial charges of each atom and for describing the electrostatic interactions. Our self-developed Pt/O/H reactive force field by D. Fantauzzi *et al.*[37] serves as atomistic potential for the platinum, the oxygenated intermediates and water, extended by the reactive force field parameters for K^+ and F^- ions.[38] There, the interactions between the electrolyte ions and water have been extensively validated while in our previous work (Ref. 37) the force field for platinum bulk and surfaces including surface oxide formation of the Pt(111) surface was intensively tested. Note, that between the charged ions and the surface no direct bonding terms are considered, as these ions are considered to keep their solvation shell. All ReaxFF calculations were performed

in the ADF software package (version 2019.103).[39,40] In general, a timestep of 0.25 fs was used for integration of the equations of motions applying the velocity-Verlet algorithm. The Nosé-Hoover thermostat with a damping constant of 100 fs set the temperature for the MD simulations at 298.15 K.[41,42] The Pt(111) surface was modelled by a symmetric twelve-layer slab ($10 \times 10 \times 12$ atoms), in which the central two layers were fixed to the corresponding calculated bulk crystal structure. Normal to the surface planes, the Pt slab is in contact with a 50 Å thick water layer ($\rho = 0.997\,\mathrm{g/cm^3}$), *e.g.* 2306 water molecules. The systems were built using the packmol software.[43] All systems presented here have been equilibrated for 400,000 iterations in the canonical NVT ensemble, followed by the production run for another 400,000 iterations. For evaluating the spatially resolved entropy of water layers Two Phase Thermodynamics (2PT) calculations have been performed, here the NVT run was followed by 50,000 iterations in the microcanonical NVE ensemble plus 5,000 iterations for evaluation within the 2PT method. For a detailed description of the method as well as the coupling between the 2PT method (developed by Lin *et al.*[44,45]) and ReaxFF we refer to our recent publication.[46] Structure visualizations were performed with the VMD software.[47]

Introducing the electrode potential in ReaxFF MD simulations

Double layer potential region

The electrified Pt(111)|H_2O interfaces have been built by appointing charges to the platinum slab, thereby premising the established conception of the free charge density being a good approximation of the electrode potential.[6,10,48] Here, Gauthier *et al.* also consider the effective free charge density as descriptor for the electrochemical driving force of processes, being preferable to the work function approach due to its sensitivity to simulation cell sizes.[48] Free charge density (denoted $\sigma_{\mathrm{Pt_{1L}}}$) describes here the actual charge located at the electrode side of the EDL, compensated by the ionic charge in the electrolyte in the absence of specific adsorption of hydrogen or hydroxide.[7,49,50] The free charge density curves obtained via

laser-induced temperature jump method by Garcia *et al.* for the Pt(111) surface in 0.1 M $HClO_4$ serve as reference for introducing the electrode potential in our simulations.[7] Note, via experimental cyclic voltammetric measurements the total charge density is accessible − including the charge transferred during adsorption processes (*e.g.* when chemical bonds are formed). In the following interfacial characterization under double layer potential conditions ($E \leq 0.5\,\mathrm{V}$), we are assuming an adsorbate free surface, therefore the equality of free charge density and total charge density holds true.

For our simulations, a series of electrified Pt(111)|water interface models have been created at different free charge densities; for charge neutrality of the double layer, $\sigma_{\mathrm{Pt_{1L}}}$ is compensated by counter ions. A detailed explanation of the methodological setup is given in the Supporting Information (SI), also describing the nature of the charges as well as their location and present counterions. Furthermore, due to the charge equilibration approach in ReaxFF the platinum atomic charges are not fixed but allowed to fluctuate (dynamically determined by the local environment), the only restriction being the imposed total charge of the slab. The resulting charge on the surface layer atoms yields a specific surface charge density corresponding to a certain electrode potential (see Fig. S2 of the SI). Depending on the electrode potential, the charge distribution within the platinum slab differs, though showing some commonalities: As can be seen in Fig. 1 (b), the main charge is located at the surface layers of the symmetrical platinum slab (denoted $\mathrm{Pt_{1L}}$). The subsequent layers show a slight Friedel oscillation, until the atomic charges deviate only marginally from the mean bulk charge.[33] To account for charge compensation of the platinum surface, counter ions, *i.e.* K^+ and F^-, are introduced to the system and are located at the outer Helmholtz plane as well as in the subsequent diffuse layer, see Fig. 1 (a).

This approach realizes a self-consistent description of the entire electrochemical interface and thus promises a more realistic ion distribution as compared to homogeneous background charges, the usage of an effective screening medium or Gaussian charge sheets as often employed in AIMD simulations.[17,20,51–53] As ReaxFF enables simulations in the nanosecond

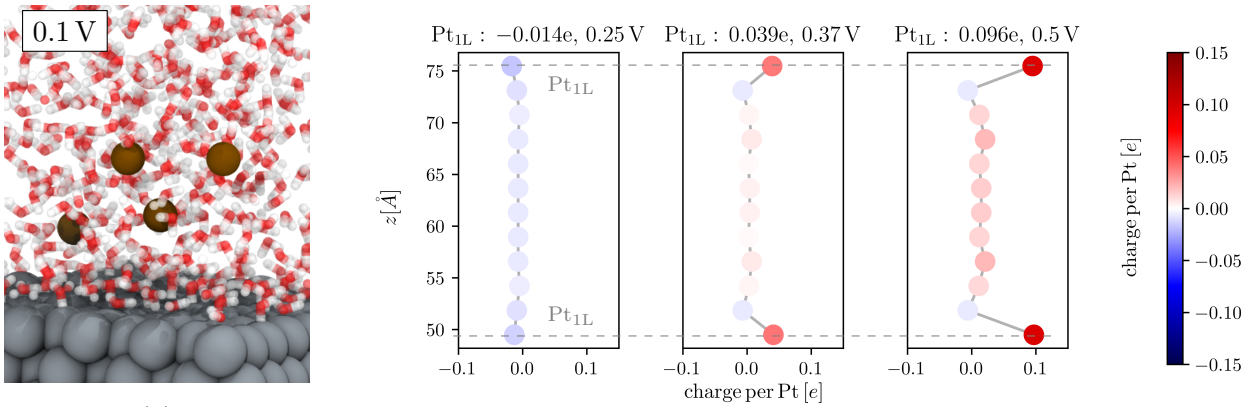

(a) (b)

Figure 1: (a) Representative snapshot of the Pt(111)|H_2O interface at a potential corresponding to 0.1 V vs. SHE. The Pt and K^+ atoms are colored in gray and brown, the water molecules are shown as red and white sticks for sake of clarity. (b) For the atomic charge distribution in the individual layers of the Pt slab, the mean atomic charge per layer is color coded between red (partially positive) and blue (partially negative). The topmost and lowest balls correspond to the surface layers (denoted: Pt_{1L}).

timescale, the interface including the ion distribution is sufficiently equilibrated, also enabling an extensive and representative sampling of the phase-space.[51]

The $\sigma_{Pt_{1L}}$ (see Fig. S2 of the SI) shows a good confirmity with the surface charge density measured by the laser-pulsed jump technique by Garcia *et al.*[7] Also, the location of zero crossing at around 0.3 V − corresponding to the point of zero free charge − is in good accordance. Tracking the evolution of the double layer charge as a function of the simulated electrode potential produces the one-humped, bell-shaped course of the double layer capacitance C_{dl}, as can be seen in the SI Fig. S2. Here, the peak around 0.3 V describes a distinct change in the double layer capacitance presumably caused by structural reorganizations of the EDL.[10,54] Especially, a potential-dependent adsorption/desorption behavior of H_2O or its orientational ordering in the interface may be of relevance here. In the following, we self-consistently investigate these characteristica in detail.

Surface oxidation potential region

In the double layer potential region, we could connect the charge density of the adsorbate-free Pt(111) surface with the electrode potential. Going to higher potentials, however, demands the consideration of appropriate adsorbate compositions (*i.e.*, oxygen atoms O*, hydroxide molecules OH* and water molecules H_2O^*) along with surface oxidation effects. In the following, a structure−potential-relation connecting a given electrode potential with the corresponding equilibrium surface structure as predicted from literature is formulated and applied. In this spirit, the theoretical studies by Kronberg *et al.*[31] and Sakong *et al.*[33] have recently included hydrogenated Pt(111) surfaces for approximation of the low potential region. So far, the authors are not aware of similar approaches for modeling the higher potential region consistently including all the relevant oxygenated adsorbates.

As taken from experimental observations (*e.g.* XPS,[1,55,56] CV[57]) and theoretical predictions,[58] OH* appears on the Pt(111) surface by H_2O oxidation from around 0.6 V onwards. This coverage becomes dominating around 0.8 V, while less H_2O^* is adsorbed on the surface. Increasing potential leads to the occurence of O* through oxidation of OH*, becoming the dominating surface species at potentials near 1 V.

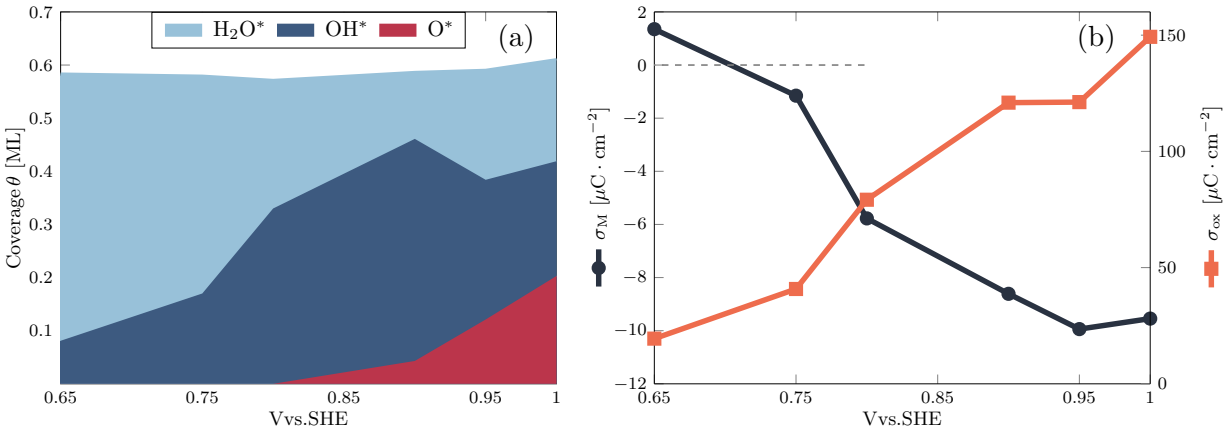

Figure 2: (a) The potential-dependent surface coverages of H_2O^*, OH* and O* are displayed as stacked area chart. The total surface coverage is observed to be around 0.6 ML throughout this potential region here. (b) The free charge density at the Platinum surface σ_M in dark blue and the charge density transferred in surface oxidation σ_{ox} in orange are displayed.

In Fig. 2 (a), the realization of the potential-dependent surface coverages in our simulations are displayed. The depicted composition of oxygenated adsorbates is thermodynamically stable and mirrors the corresponding electrochemical environment at the respective electrode potential, without including the potential as an explicit parameter of the simulation. The total coverage of OH^*, H_2O^* and O^* is around 0.6 ML over the whole potential range. This resembles the coverage as known from traditional water bilayer models, demanding an intensive structural elucidation of the hydrogen bonding present and adsorbate configurations (see results section). For a description of the location of charges and the total amount of K^+ and F^- ions, see the SI.

For verifying our structure−potential-relation the structural model of the electrified Pt(111) interface by Huang *et al.* serves as benchmark.[59] Within their model, the authors include parameter-based submodels for an oxide layer, the water layer and the diffuse layer. They are consequently able to deconvolute the total charge density into contributions arising from Pt oxidation (σ_{ox}) or hydrogen adsorption and the free surface charge density σ_M. σ_M itself is associated to the dipole moment of the oxide layer, the water dipole in the interfacial electric field and the pure double-layer charging. In our simulations, the deconvolution is not required as the interface is treated self-consistently. We calculate σ_M as the charge density of the Pt surface layer including the partial charges of oxygenated intermediates and adsorbed H_2O^* molecules. Correlating the respective surface coverages of OH^*, H_2O^* and O^* to the expected number of transferred electrons upon adsorption, σ_{ox} is obtained. Here, we can reproduce the course of σ_M in the structural model by Huang *et al.* along with the location of zero-crossing, as well as the magnitude of the charge density in the potential range between 0.65 and 1.0 V, see Fig. 2 (b).

We have presented two approaches to include the effects of an electrode potential into ReaxFF simulations: First, the double layer potential region (up to 0.5 V) is installed over the potential-defining free charge densities on the adsorbate-free Pt(111) surface. Second, in the surface oxidation potential region (0.65−1.0 V) the stable coverages of oxygenated

intermediates on the Pt(111) surface define the free surface charge density and correlate to a specific electrode potential.

Results and Discussion

The orientation of the interfacial water molecules is influenced by the chemical interactions between platinum and water, the free charge density (affecting the direction of the water dipoles) as well as the presence of adsorbates (through blocking of sites and manipulating the electrostatic effect of the free charge density). Here, three main configurations of interfacial water can be distinguished: H_2O-parallel, with the molecule adsorbed via the oxygen atom on a top-site of the Pt surface and both hydrogen atoms slightly tilted away from the surface. H-up, where one hydrogen atom points away from the surface and H-down with one hydrogen atom directed towards the surface, see Fig. 3 for visualization. Numerous studies have contributed here, obtaining small to negligible differences in stability between the two orientations.[25,27,60–63] In the following, we focus on − with no claim to completeness − experimental and theoretical work including the electrode potential into their investigation of the Pt|H_2O interface. In our ReaxFF-MD study, we observe a change of the preferred orientation of interfacial H_2O from H-up to H-down with increasing electrode potential. To the author's knowledge, this shift to a dominating H-down configuration in the surface oxidation potential region is so far undocumented. A detailed discussion of the structure of the water layer as well as the occurrence of ordered patterns will be presented together with the spatially-resolved entropy behavior later. Near the assumed location of the potential of zero charge (*pzc*, ∼0.3 V), both H-up and H-down orientations of the interfacial water molecules (*e.g.* H_2O within 3.5 Å distance to the Pt surface) are observed. In Fig. 3, this is represented by a comparable proportion of both configurations. Up to 0.5 V, the H-up orientation is distinctly preferred, in line with AIMD studies.[10,11,31] This indicates a strong correlation between the water orientation and the free charge density, as with a more

positively charged surface the hydrogen atoms tend to point away from the surface.

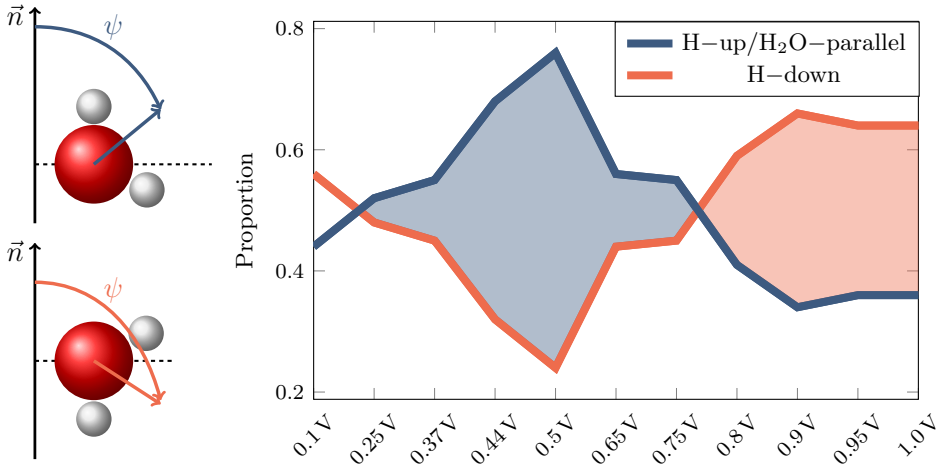

Figure 3: Depending on the applied electrode potential, the orientation of the adsorbed water molecules on the Pt(111) surface is categorized as H-down or H-up/H_2O-parallel. Hereby, H-down corresponds to one hydrogen atom pointing towards the surface characterized by an angle $\psi > 90\,^\circ$ between the surface normal vector $\vec{n}$ and the water bisector vector. Analogously, H-up corresponds to one hydrogen atom pointing away from the Pt surface and an angle $\psi < 90\,^\circ$. Shaded areas in the plot correspond to the dominating configuration in the respective potential region.

Also, the surface coverage of H_2O^* is increasing in this potential region, up to 0.76 ML at 0.5 V. Following Le *et al.*'s argumentation, this increase in coverage induces a significant interface dipole potential change and causes a negative capacitance.[10] This is in line with the obtained one-humped course of the differential double layer capacitance with its maximum near the *pzc* as depicted in Fig. S2 of the SI. Singular occurrences of H_2O^* dissociation, leading to H^* and OH^* can be detected. However, as soon as oxygenated intermediates are present on the Pt(111) surface, the proportion of H-down oriented H_2O^* is increasing and from 0.8 V onwards dominating. The presence of negatively charged adsorbates (*e.g.* OH^* and O^*) promotes the reorientation of interfacial water molecules to pointing their positive charges on the hydrogen atoms towards the surface. This is visualized in Fig. 3, where the H-down configuration is observed for up to 66 % of the interfacial water molecules between 0.9 V and 1.0 V. The median of the angle ψ between the water bisector vector and the

surface supports additionally our observation of the preference of the H-down configuration with increasing potential: ψ_{median} is changing from 61.7 ° at 0.44 V to its maximum value of 105.2 ° at 1.0 V. This reorientation is however restricted to the water molecules within a few Ångströms distance to the Pt(111) surface. Further away from the platinum surface, the water molecules shows random orientations and are only locally affected by charged ions. For a detailed study of the ion−water interaction the reader is referred to Ref. 38. As the orientation of the interfacial water molecules is a result of several (competing) influences, we expect the intermolecular ordering and hydrogen bonded network to be affected as well. For elucidation thereof, we investigated the course of the water's entropy at the Pt(111) interface in combination with the distribution profiles of water regarding the Pt−H_2O distance and the H_2O^*−H_2O^* in-plane distances.

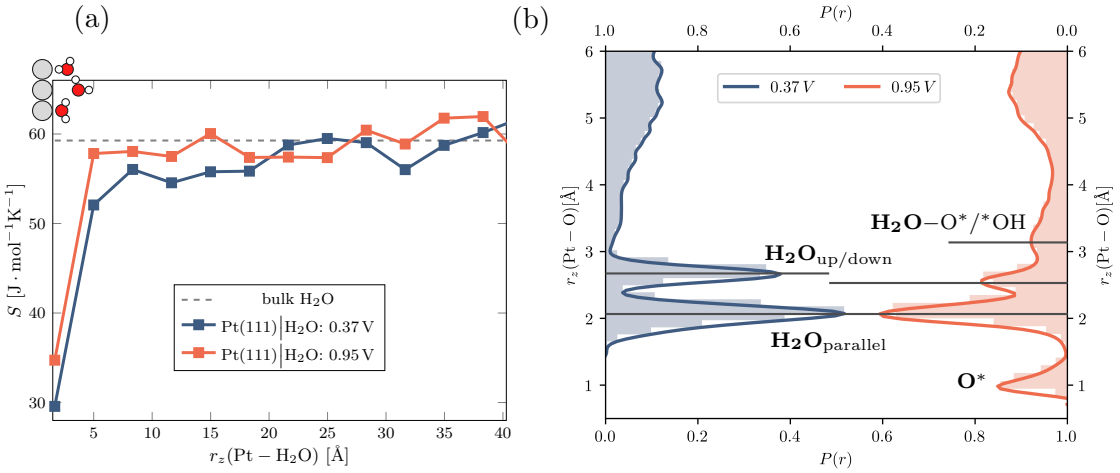

Figure 4: Variations on the electrode potential affect the thermodynamics of the Pt|H_2O interface. In (a), the course of the entropy S for two simulated electrode potentials with increasing distance from the Pt(111) surface is depicted. Each data point has been calculated in a water layer of $\Delta z = 3.3$ Å. The dashed line represents the average H_2O bulk value of the entropy, 59.27 J/molK.[46] (b) Oxygen distribution in z direction with increasing distance from the Pt surface for 0.37 V and 0.95 V electrode potential. Characteristic Pt−H_2O distances are labelled for comparison.

We have successfully transferred the Two Phase Thermodynamics method (2PT) to the ReaxFF framework and the Pt(111)|H_2O interface for a structural and thermodynamical characterization thereof, see Ref. 46. This method constitutes the calculation of thermody-

namical quantities by merely post-processing a molecular dynamics trajectory, dividing the density of states function of the liquid into a superposition of solid and diffusive contributions and thereon applying the respective thermodynamic theories. There, we have observed a significant reduction of the entropy S by nearly 50 % in the adsorbed water layer on the Pt(111) surface at conditions of potential of zero charge compared to the entropy in bulk water. The bulk water entropy has been determined as $S_{\mathrm{H_2O,\,bulk}} = 59.27\,\mathrm{J/molK}$, deviating by 15 % from the experimental value of $S_{\mathrm{H_2O,\,exp}} = 69.95\,\mathrm{J/molK}$.[64] This underestimation occurs over several empirical water models, the main reason being too stiff hydrogen bonding interactions, and has been discussed in detail in our recent work.[46] In Fig. 4 (a), the potential-dependent evolution of the entropy from the adsorbed water layer into the bulk water is depicted. For the double layer potential region in general and exemplary at $E = 0.37\,\mathrm{V}$, the reduced entropy of $S_{\mathrm{H_2O^*,\,0.37\,V}} = 29.57\,\mathrm{J/molK}$ (compared to the bulk water entropy of $S_{\mathrm{H_2O,\,bulk}} = 59.27\,\mathrm{J/molK}$) suggests a higher ordering in the H_2O^* adsorbate layer. This can be structurally resolved to the occurrence of (disordered patterns of) five-, six-, or seven-membered rings. However, due to the dynamics and thermal fluctuations, no ideal hexagonal hydrogen-bonded network can be observed. The effect of the charged platinum electrode onto the water's entropy lasts up to a distance of $15-20\,\mathrm{Å}$, then the entropy fluctuates around the bulk value of $S_{\mathrm{H_2O,\,bulk}}$. This observation is however dependent on the potential: From $0.1-0.5\,\mathrm{V}$, the entropy reducing range of the Pt surface is increasing. The simultaneously growing proportion of H-up configurations of H_2O^* enables the formation of hydrogen bonds between the layer of adsorbed water molecules and the subsequent wetting layers. In contrast, under surface oxidation potential conditions the water's entropy regains its bulk value directly after the layer of adsorbed water ($S_{\mathrm{H_2O^*,\,0.95\,V}} = 34.73\,\mathrm{J/molK}$). Here, the dominating H-down configuration induces hydrophobicity, as hydrogen bonding within the H_2O^* layer is encouraged while less hydrogen bonds are donated to the surrounding bulk water.[65]

This can be also interpreted from Fig. 4 (b) where the oxygen distribution with increasing dis-

tance to the Pt(111) surface is shown. While in the double layer potential region ($E \leq 0.5\,\mathrm{V}$) only H_2O^* is present at the surface, producing two distinctive peaks of 2.1 Å and 2.65 Å, the distribution profile differs in the surface oxidation potential region ($E = 0.65 - 1.0\,\mathrm{V}$): Here, additional peaks for O^* at 1.05 Å and for H_2O molecules hydrogen bonded to O^* or OH^* at $\sim$3.1 Å appear. Depending on the respective local environment, the H-up or H-down configurations are located a bit closer to the Pt(111) surface. Subsequently at around 3−4 Å, a nearly depleted region (*e.g.* low density area) contains mainly dangling hydrogen bonds. The width of this depleted region is again influenced by the applied electrode potential, spanning 1.6 Å at 0.1 V to only 0.8 Å at 0.5 V. Here, a balanced H-up/H-down proportion enables the formation of an intact intra- (*e.g.* within the adsorbed water layer) and interlayer (*e.g.* bridging the depleted region) hydrogen bond network (typical hydrogen bond length: 1.8 Å). Meanwhile, an increasing occurrence of H_2O_{parallel} or H-up configurations comprises the network and reduces the extent of layering in z direction. In the surface oxidation potential region, due to the presence of oxygenated intermediates, the water layer is less homogeneous reflected by a less prominent adjacent depleted region and a more disconnected hydrogen bond network.

Lastly, to further elucidate the correlation between the entropy and structural ordering of water molecules on the Pt(111) surface, the $H_2O^*-H_2O^*$ distance distribution is evaluated. Here, the occurring distances are compared to the discrete distances of an ideal hexagonal water network, see Fig. S3 in the SI, as well as Figs. S4 and S5. In the double layer potential region, a distinct in-plane ordering of the adsorbed water molecules can be observed. With increasing potential though, a broadening of the peaks introduces noise, suggesting a less distinct ordering. This can be also traced back to the increasing coverage of H_2O^*, surpassing the coverage of the ideal hexagonal adsorbate structure (2/3 ML) at 0.37 V. For the surface oxidation potential region, the presence of O^* is deciding: For $E < 0.9\,\mathrm{V}$, only OH^* and H_2O^* are present on the surface, which are maintaining a fairly ordered hydrogen bonded network, represented by discrete peaks in the O−O distance distribution. The presence of O^* however

seriously disturbs the ordering on the surface and causes a broadening of the O−O distance distribution. In the water layer beyond the depleted region, in a distance of $\sim 4 - 6.5\,\text{Å}$ to the Pt(111) surface, no ordering kann be observed − independent of the applied potential. This is interpreted from a smooth distribution of the O−O distance distribution in Fig. S3 (right) of the SI, featuring no distinct peaks as known from hexagonal motifs.

Conclusion

In the present work we present a self-consistent approach to handle the electrode potential in electrochemical interfaces, based on the bond-order dependent ReaxFF force field molecular dynamics approach. This method was applied to describe the electrochemical interface between a Pt(111) electrode and different aqueous electrolytes, with a particular focus on the structure and properties of the predominant water within the interface region as function of the electrode potential. Here, the potential within the double layer region ($E < 0.5\,\text{V}$) is reproduced by imposing a charge on the platinum slab, mirroring the free charge density on the surface as known from experimental studies. For the surface oxidation potential region ($E = 0.65 - 1.0\,\text{V}$), the compositions of oxygenated intermediates on the Pt(111) surface (*e.g.* O^*, OH^*, H_2O^*) as known from literature are adapted and kept during the simulations, thereby premising a structure−potential-relation. Subsequently, the potential-dependent orientation of interfacial water is investigated, obtaining a shift of preference to H-down oriented adsorbed water in the surface oxidation potential region, due to the presence of oxygenated adsorbates. For investigation of the intermolecular water ordering and the hydrogen bonded network, the spatially resolved entropy of the water layers is calculated via the Two Phase Thermodynamics approach, which we have recently adapted to the ReaxFF force field framework.[46] An enhanced ordering effect can be observed in the double layer potential region, where a balanced proportion of H-up and H-down configuration proves beneficial. Furthermore, our studies shed light on the interplay between water as

electrolyte and the Pt(111) electrode, including the electrode potential, adsorbates and ions contributing to its still ongoing characterization and understanding process. As our approach realizes a self-consistent treatment of the electrochemical interface, our work demonstrates the capabilities of the ReaxFF method for the further clarification of the interface between electrode and electrolyte as well as the further optimization of electrochemical processes in heterogeneous catalysis.

Acknowledgement

This research was conducted as part of the German Research Foundation (DFG) under Project ID 390874152 (POLiS Cluster of Excellence) as well as the Sonderforschungsbereiche (collaborative research centers) SFB-1316 and SFB-1249. In addition, support from the BMBF (Bundesministerium für Bildung und Forschung) through the project InnoSüd (Grant Agreement: 03IHS024D) is gratefully acknowledged. Further, the authors acknowledge the computer time supported by the state of Baden-Württemberg through the bwHPC project and the DFG through grant number INST40/ 467-1 FUGG. The authors express their thanks to Andrey Sinyavskiy for coupling the 2PT method with ReaxFF and to Dr. Ludwig Kibler for fruitful discussions, sharing his impressive knowledge and asking the right questions.

Supporting Information

S1: Location of Charge in the potential-dependent MD simulations

The electrified Pt(111)|water interface models have been built either by establishing a certain free charge density on the Pt surface ($\sigma_{\mathrm{Pt_{1L}}}$) corresponding to a certain potential ($E \leq 0.5\,\mathrm{V}$) or by following a structure−potential-relation and setting up the thermodynamically stable adsorbate composition on the surface ($E \geq 0.65\,\mathrm{V}$).

Table S1: Parameters for establishing the electrified models of the Pt(111)|interfaces: Charges imposed on the platinum slab ($\sum q_{\mathrm{Pt}}$) for the respective potential and the obtained charge densities $\sigma_{\mathrm{Pt_{1L}}}$ or σ_{M}, complemented by the number of ions in the system.

Potential [V]	$\sum q_{\mathrm{Pt}}$ $[e]$ [a]	$\sigma_{\mathrm{Pt_{1L}}}$ $[\mu\mathrm{C}\cdot\mathrm{cm}^{-2}]$	ions
0.1	−20	−10.31	12 K^+
0.25	−10	−3.19	4 K^+
0.37	10	9.71	8 F^-
0.44	20	16.44	18 F^-
0.5	30	22.94	24 F^-
		σ_{M} $[\mu\mathrm{C}\cdot\mathrm{cm}^{-2}]$	
0.65		1.35	
0.75		−1.15	
0.8		−5.77	6 K^+, 6 F^-
0.9		−8.61	8 K^+, 8 F^-
0.95		−9.94	10 K^+, 10 F^-
1.0		−9.94	10 K^+, 10 F^-

[a] The sum of the atomic charge of the 1200 Pt atoms in the systems must equal $\sum q_{\mathrm{Pt}}$ during the whole simulation.

In the double layer potential region, the free charge density corresponds to a certain surface charge and charge distribution in the platinum slab. In Table S1, the charges imposed on the platinum slab in total are specified. Note, that the complete charge has been predefined, while the local atomic environment of the platinum and the surrounding water determine the atomic charges (within the slab and especially on the Pt surface layer) and the resulting charge density is connected to an electrode potential. In this sense, $\sigma_{\mathrm{Pt_{1L}}}$ is

then compensated by counterions to account for charge neutrality of the double layer. This is visualized exemplary in Fig. S1 for a simulated potential of 0.25 V. Here, however, needs to be noted that some simulation cells are not charge neutral, as the number of ions does not equal the charge on the platinum slab. This arises due to the fitting of the number of ions to compensate the free charge density $\sigma_{\mathrm{Pt_{1L}}}$ rather than the charge within the platinum slab. Altogether, the most realistic courses of the double layer charge were obtained with the systems defined in table S1, besides, ReaxFF is capable of handling charged systems without limitations.

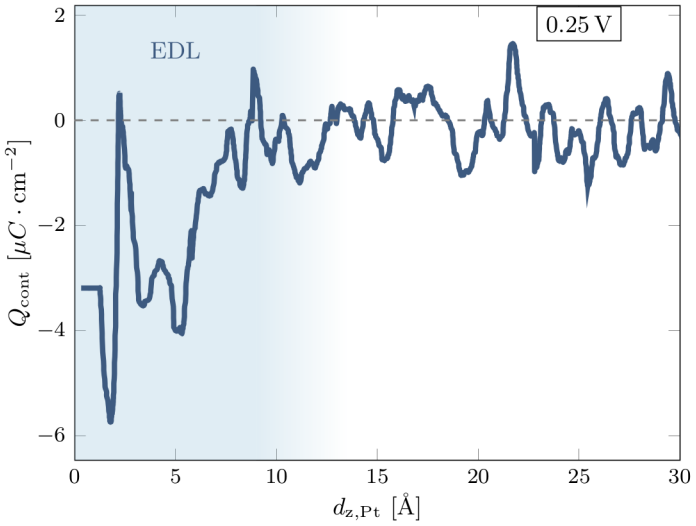

Figure S1: The course of the continuous charge with increasing distance from the Pt(111) surface ($d_{\mathrm{z,Pt}}$) is shown. On the left, the curve starts with the platinum surface charge density, the peaks correspond to the layer of adsorbed water, then, subsequently, neutrality is reached at ∼12 Å.

In the surface oxidation potential region, no charge restraints need to be imposed on the system and the simulation cells are charge neutral. To establish the electrode potential, the experimentally observed and thermodynamically stable compositions of oxygenated adsorbates are installed on the platinum surface. Therefore, the respective number of ions (both K^+ and F^-) to match the free surface charge density σ_{M} are added to the system, see table S1. Also, the adsorbates on the Pt(111) surface and the H_2O molecules in the liquid carry

charge: If OH^* is present on the surface, it is partially charged with $-0.16 \pm 0.03\,e$ along with atomic oxygen O^* carrying a partial negative charge of $-0.3\,e$. Those are compensated by a negligible mean charge on the H_2O molecules in the water environment of around $0.005\,e$. Negligible because hydrogen bonding induces partial charging of up to $\pm 0.05\,e$ on water molecules.

S2: Determination of the Double Layer Capacitance

In the double layer potential region, the surface charge density of the platinum surface ($\sigma_{\mathrm{Pt_{1L}}}$) serves as linker to the electrode potential in our simulations, see Fig. S2. From these MD simulations, the double layer charge C_{dl} has been determined (see Fig. S1). The differential double layer capacitance C_{dl} is calculated as

$$C_{\mathrm{dl}} = \frac{Q_{\mathrm{dl}}}{\mathrm{d}V} \tag{1}$$

and shown in Fig. S2. Measurements of the double layer capacitance as obtained from electrochemical impedance experiments show a maximum around 0.3 V, which can be reproduced with our ReaxFF MD simulations.

S3: Ordering within the layer of adsorbed water

The intermolecular $H_2O^*-H_2O^*$ distance distribution, measured via the O−O distances, can give valuable insights into the ordering within the layer of adsorbed water. Comparing the potential-dependent distance distribution with the discrete distances appearing in a perfectly ordered, hexagonal hydrogen-bonded water network enables drawing conclusions regarding the degree of ordering of the H_2O^* on the platinum surface. In Fig. S3 (left), the distributions for the intermolecular H_2O^* distances are compared for a representative double layer potential (0.37 V) and a surface oxide potential (0.95 V). In the subsequent wetting layer, corresponding to H_2O molecules above the depleted region in 4−6.5 Å distance to the

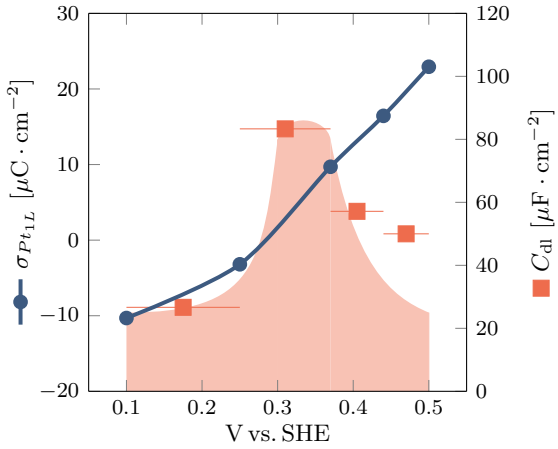

Figure S2: The free charge density on the Pt(111) surface in dark blue and the obtained double layer capacitance for the Pt(111)|water interface in orange marks are shown. The horizontal lines show the potential range dV for calculation of C_{dl}. The filled one-humped form is based on Ref. 66.

Pt surface, no characteristic peaks for discrete hexagonal distances can be detected. Thereby, independent of the potential, no ordering is observable within the water layers beyond the depleted region.

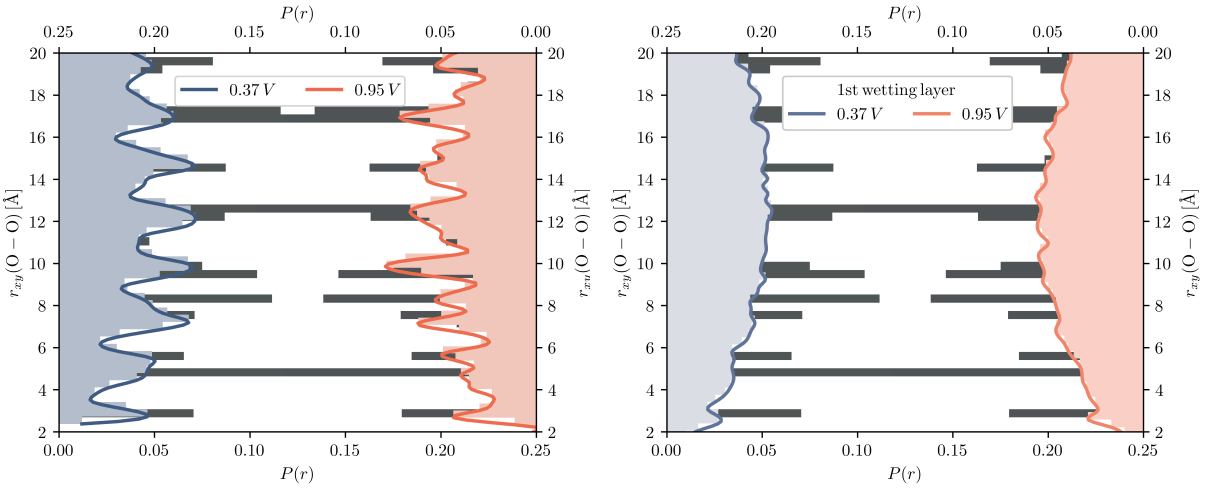

Figure S3: Distributions of the oxygen-oxygen in-plane distance (x,y direction) for the adsorbed H_2O^* at the Pt(111) surface (left) and for H_2O within 4 − 6.5 Å distance to the Pt(111) surface (right) for two electrode potentials. The gray bars correspond to O−O distances calculated from an ideal hexagonal water network, adsorbed on Pt(111). The blue and orange bars have been obtained from and averaged over five independent MD-simulations.

The distance distributions for the layer of adsorbed water molecules for 0.75 V and 0.8 V

are displayed in Fig. S4, complemented by those for the remaining potentials investigated between 0.1 V and 0.5 V in Fig. S5.

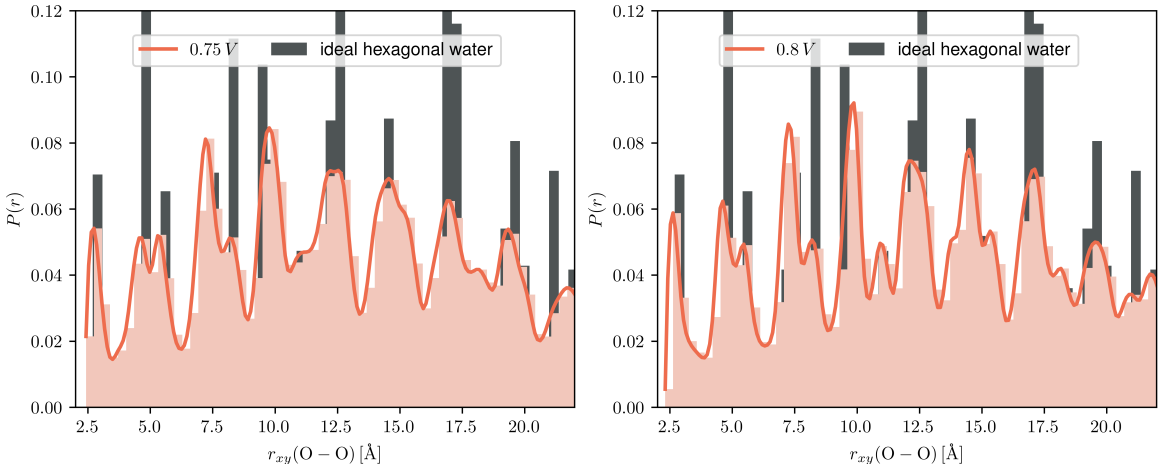

Figure S4: Distributions of the oxygen-oxygen in-plane distance (x,y direction) for the adsorbed H_2O^* at the Pt(111) surface for electrode potentials of 0.75 V and 0.8 V. The gray bars correspond to O−O distances calculated from an ideal hexagonal water network, adsorbed on Pt(111). The blue and orange bars have been obtained from and averaged over five independent MD-simulations.

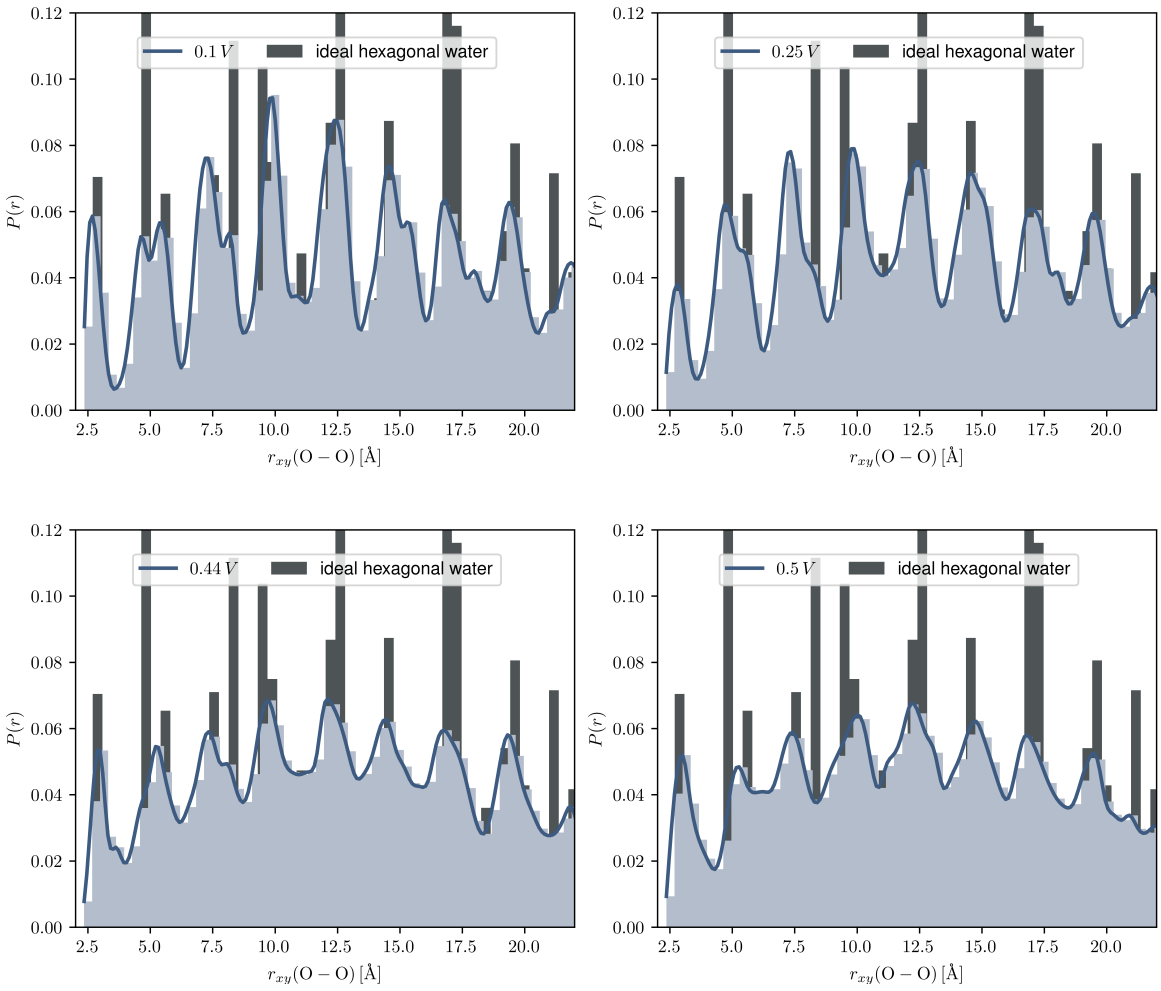

Figure S5: Distributions of the oxygen-oxygen in-plane distance (x,y direction) for the adsorbed H_2O^* at the Pt(111) surface for electrode potentials of 0.1 V, 0.25 V, 0.44 V and 0.5 V. The gray bars correspond to O−O distances calculated from an ideal hexagonal water network, adsorbed on Pt(111). The blue and orange bars have been obtained from and averaged over five independent MD-simulations.

References

(1) Casalongue, H. S.; Kaya, S.; Viswanathan, V.; Miller, D. J.; Friebel, D.; Hansen, H. A.; Nørskov, J. K.; Nilsson, A.; Ogasawara, H. Direct observation of the oxygenated species during oxygen reduction on a platinum fuel cell cathode. *Nature Communications* **2013**, *4*, 2817.

(2) Ledezma-Yanez, I.; Wallace, W. D. Z.; Sebastián-Pascual, P.; Climent, V.; Feliu, J. M.; Koper, M. T. M. Interfacial water reorganization as a pH-dependent descriptor of the hydrogen evolution rate on platinum electrodes. *Nature Energy* **2017**, *2*, 17031.

(3) Bella, F.; Gerbaldi, C.; Barolo, C.; Grätzel, M. Aqueous dye-sensitized solar cells. *Chem. Soc. Rev.* **2015**, *44*, 3431–3473.

(4) Xu, S.; Carter, E. A. Theoretical Insights into Heterogeneous (Photo)electrochemical CO2 Reduction. *Chemical Reviews* **2019**, *119*, 6631–6669, PMID: 30561988.

(5) Shi, H.; Poudel, N.; Hou, B.; Shen, L.; Chen, J.; Benderskii, A. V.; Cronin, S. B. Sensing local pH and ion concentration at graphene electrode surfaces using in situ Raman spectroscopy. *Nanoscale* **2018**, *10*, 2398–2403.

(6) Li, C.-Y.; Le, J.-B.; Wang, Y.-H.; Chen, S.; Yang, Z.-L.; Li, J.-F.; Cheng, J.; Tian, Z.-Q. In situ probing electrified interfacial water structures at atomically flat surfaces. *Nature Materials* **2019**, *18*, 697–701.

(7) Garcia-Araez, N.; Climent, V.; Feliu, J. Potential-Dependent Water Orientation on Pt(111), Pt(100), and Pt(110), As Inferred from Laser-Pulsed Experiments. Electrostatic and Chemical Effects. *The Journal of Physical Chemistry C* **2009**, *113*, 9290–9304.

(8) Ojha, K.; Arulmozhi, N.; Aranzales, D.; Koper, M. T. M. Double Layer at the Pt(111)–Aqueous Electrolyte Interface: Potential of Zero Charge and Anomalous

Gouy–Chapman Screening. *Angewandte Chemie International Edition* **2020**, *59*, 711–715.

(9) Schultz, Z. D.; Shaw, S. K.; Gewirth, A. A. Potential Dependent Organization of Water at the Electrified Metal Liquid Interface. *Journal of the American Chemical Society* **2005**, *127*, 15916–15922, PMID: 16277535.

(10) Le, J.-B.; Fan, Q.-Y.; Li, J.-Q.; Cheng, J. Molecular origin of negative component of Helmholtz capacitance at electrified Pt(111)/water interface. *Science Advances* **2020**, *6*.

(11) Sakong, S.; Groß, A. Water structures on a Pt(111) electrode from ab initio molecular dynamic simulations for a variety of electrochemical conditions. *Phys. Chem. Chem. Phys.* **2020**, *22*, 10431–10437.

(12) Magnussen, O. M.; Groß, A. Toward an Atomic-Scale Understanding of Electrochemical Interface Structure and Dynamics. *Journal of the American Chemical Society* **2019**, *141*, 4777–4790, PMID: 30768905.

(13) Bjorneholm, O.; Hansen, M. H.; Hodgson, A.; Liu, L.-M.; Limmer, D. T.; Michaelides, A.; Pedevilla, P.; Rossmeisl, J.; Shen, H.; Tocci, G.; Tyrode, E.; Walz, M.-M.; Werner, J.; Bluhm, H. Water at Interfaces. *Chemical Reviews* **2016**, *116*, 7698–7726, PMID: 27232062.

(14) Nørskov, J. K.; Rossmeisl, J.; Logadottir, A.; Lindqvist, L.; Kitchin, J. R.; Bligaard, T.; Jónsson, H. Origin of the Overpotential for Oxygen Reduction at a Fuel-Cell Cathode. *The Journal of Physical Chemistry B* **2004**, *108*, 17886–17892.

(15) Lozovoi, A. Y.; Alavi, A.; Kohanoff, J.; Lynden-Bell, R. M. Ab initio simulation of charged slabs at constant chemical potential. *The Journal of Chemical Physics* **2001**, *115*, 1661–1669.

(16) Bouzid, A.; Pasquarello, A. Atomic-Scale Simulation of Electrochemical Processes at Electrode/Water Interfaces under Referenced Bias Potential. *The Journal of Physical Chemistry Letters* **2018**, *9*, 1880–1884, PMID: 29589437.

(17) Bouzid, A.; Gono, P.; Pasquarello, A. Reaction pathway of oxygen evolution on Pt(111) revealed through constant Fermi level molecular dynamics. *Journal of Catalysis* **2019**, *375*, 135–139.

(18) Liang, T.; Antony, A. C.; Akhade, S. A.; Janik, M. J.; Sinnott, S. B. Applied Potentials in Variable-Charge Reactive Force Fields for Electrochemical Systems. *The Journal of Physical Chemistry A* **2018**, *122*, 631–638, PMID: 29257690.

(19) Otani, M.; Hamada, I.; Sugino, O.; Morikawa, Y.; Okamoto, Y.; Ikeshoji, T. Structure of the water/platinum interface—a first principles simulation under bias potential. *Phys. Chem. Chem. Phys.* **2008**, *10*, 3609–3612.

(20) Taylor, C. D.; Wasileski, S. A.; Filhol, J.-S.; Neurock, M. First principles reaction modeling of the electrochemical interface: Consideration and calculation of a tunable surface potential from atomic and electronic structure. *Phys. Rev. B* **2006**, *73*, 165402.

(21) Bonnet, N.; Marzari, N. First-Principles Prediction of the Equilibrium Shape of Nanoparticles Under Realistic Electrochemical Conditions. *Phys. Rev. Lett.* **2013**, *110*, 086104.

(22) Sakong, S.; Naderian, M.; Mathew, K.; Hennig, R. G.; Groß, A. Density functional theory study of the electrochemical interface between a Pt electrode and an aqueous electrolyte using an implicit solvent method. *The Journal of Chemical Physics* **2015**, *142*, 234107.

(23) Tripkovic, V.; Björketun, M. E.; Skúlason, E.; Rossmeisl, J. Standard hydrogen electrode and potential of zero charge in density functional calculations. *Phys. Rev. B* **2011**, *84*, 115452.

(24) Skúlason, E.; Karlberg, G. S.; Rossmeisl, J.; Bligaard, T.; Greeley, J.; Jónsson, H.; Nørskov, J. K. Density functional theory calculations for the hydrogen evolution reaction in an electrochemical double layer on the Pt(111) electrode. *Phys. Chem. Chem. Phys.* **2007**, *9*, 3241–3250.

(25) Schnur, S.; Groß, A. Properties of metal–water interfaces studied from first principles. *New Journal of Physics* **2009**, *11*, 125003.

(26) Nie, S.; Feibelman, P. J.; Bartelt, N. C.; Thürmer, K. Pentagons and Heptagons in the First Water Layer on Pt(111). *Phys. Rev. Lett.* **2010**, *105*, 026102.

(27) Feibelman, P. J.; Bartelt, N. C.; Nie, S.; Thürmer, K. Interpretation of high-resolution images of the best-bound wetting layers on Pt(111). *The Journal of Chemical Physics* **2010**, *133*, 154703.

(28) Hansen, M. H.; Jin, C.; Thygesen, K. S.; Rossmeisl, J. Finite Bias Calculations to Model Interface Dipoles in Electrochemical Cells at the Atomic Scale. *The Journal of Physical Chemistry C* **2016**, *120*, 13485–13491.

(29) Bellarosa, L.; García-Muelas, R.; Revilla-López, G.; López, N. Diversity at the Water–Metal Interface: Metal, Water Thickness, and Confinement Effects. *ACS Central Science* **2016**, *2*, 109–116, PMID: 26937488.

(30) Kristoffersen, H. H.; Vegge, T.; Hansen, H. A. OH formation and H2 adsorption at the liquid water–Pt(111) interface. *Chem. Sci.* **2018**, *9*, 6912–6921.

(31) Kronberg, R.; Laasonen, K. Coupling Surface Coverage and Electrostatic Effects on the Interfacial Adlayer–Water Structure of Hydrogenated Single-Crystal Platinum Electrodes. *The Journal of Physical Chemistry C* **2020**, *124*, 13706–13714.

(32) Roman, T.; Groß, A. Structure of water layers on hydrogen-covered Pt electrodes. *Catalysis Today* **2013**, *202*, 183–190, Electrocatalysis.

(33) Sakong, S.; Groß, A. The electric double layer at metal-water interfaces revisited based on a charge polarization scheme. *The Journal of Chemical Physics* **2018**, *149*, 084705.

(34) van Duin, A. C. T.; Dasgupta, S.; Lorant, F.; A., G. W. ReaxFF: A Reactive Force Field for Hydrocarbons. *Journal of Physical Chemistry A* **2001**, *105*, 9396–9409.

(35) Chenoweth, K.; van Duin, A. C. T.; Goddard, W. A. ReaxFF Reactive Force Field for Molecular Dynamics Simulations of Hydrocarbon Oxidation. *The Journal of Physical Chemistry A* **2008**, *112*, 1040–1053.

(36) Mortier, W. J.; Ghosh, S. K.; Shankar, S. Electronegativity-equalization method for the calculation of atomic charges in molecules. *Journal of the American Chemical Society* **1986**, *108*, 4315–4320.

(37) Fantauzzi, D.; Bandlow, J.; Sabo, L.; Mueller, J. E.; van Duin, A. C. T.; Jacob, T. Development of a ReaxFF potential for Pt–O systems describing the energetics and dynamics of Pt-oxide formation. *Phys. Chem. Chem. Phys.* **2014**, *16*, 23118–23133.

(38) Fedkin, M. V.; Shin, Y. K.; Dasgupta, N.; Yeon, J.; Zhang, W.; van Duin, D.; van Duin, A. C. T.; Mori, K.; Fujiwara, A.; Machida, M.; Nakamura, H.; Okumura, M. Development of the ReaxFF Methodology for Electrolyte–Water Systems. *The Journal of Physical Chemistry A* **2019**, *123*, 2125–2141, PMID: 30775922.

(39) te Velde, G.; Bickelhaupt, F. M.; Baerends, E. J.; Fonseca Guerra, C.; van Gisbergen, S. J. A.; Snijders, J. G.; Ziegler, T. Chemistry with ADF. *Journal of Computational Chemistry* **2001**, *22*, 931–967.

(40) Baerends, E. J. et al. ADF2017, SCM, Theoretical Chemistry, Vrije Universiteit, Amsterdam, The Netherlands, https://www.scm.com.

(41) Nosé, S. A unified formulation of the constant temperature molecular dynamics methods. *The Journal of Chemical Physics* **1984**, *81*, 511–519.

(42) Hoover, W. G. Canonical dynamics: Equilibrium phase-space distributions. *Phys. Rev. A* **1985**, *31*, 1695–1697.

(43) Martínez, L.; Andrade, R.; Birgin, E. G.; Martínez, J. M. PACKMOL: A package for building initial configurations for molecular dynamics simulations. *Journal of Computational Chemistry* **2009**, *30*, 2157–2164.

(44) Lin, S.-T.; Blanco, M.; Goddard, W. A. The two-phase model for calculating thermodynamic properties of liquids from molecular dynamics: Validation for the phase diagram of Lennard-Jones fluids. *The Journal of Chemical Physics* **2003**, *119*, 11792–11805.

(45) Lin, S.-T.; Maiti, P. K.; Goddard, W. A. Two-Phase Thermodynamic Model for Efficient and Accurate Absolute Entropy of Water from Molecular Dynamics Simulations. *The Journal of Physical Chemistry B* **2010**, *114*, 8191–8198, PMID: 20504009.

(46) Jung, C. K.; Braunwarth, L.; Sinyavskiy, A.; Jacob, T. Thermodynamic Description of Interfaces applying the 2PT method on ReaxFF Molecular Dynamics simulations. 2021.

(47) Humphrey, W.; Dalke, A.; Schulten, K. VMD – Visual Molecular Dynamics. *Journal of Molecular Graphics* **1996**, *14*, 33–38.

(48) Gauthier, J. A.; Dickens, C. F.; Heenen, H. H.; Vijay, S.; Ringe, S.; Chan, K. Unified Approach to Implicit and Explicit Solvent Simulations of Electrochemical Reaction Energetics. *Journal of Chemical Theory and Computation* **2019**, *15*, 6895–6906, PMID: 31689089.

(49) Climent, V.; Attard, G.; Feliu, J. Potential of zero charge of platinum stepped surfaces: a combined approach of CO charge displacement and N2O reduction. *Journal of Electroanalytical Chemistry* **2002**, *532*, 67–74.

(50) Frumkin, A.; Petrii, O. Potentials of zero total and zero free charge of platinum group metals. *Electrochimica Acta* **1975**, *20*, 347–359.

(51) Abidi, N.; Lim, K. R. G.; Seh, Z. W.; Steinmann, S. N. Atomistic modeling of electrocatalysis: Are we there yet? *WIREs Computational Molecular Science* **2020**, *n/a*, e1499.

(52) Otani, M.; Sugino, O. First-principles calculations of charged surfaces and interfaces: A plane-wave nonrepeated slab approach. *Phys. Rev. B* **2006**, *73*, 115407.

(53) Lozovoi, A. Y.; Alavi, A. Reconstruction of charged surfaces: General trends and a case study of Pt(110) and Au(110). *Phys. Rev. B* **2003**, *68*, 245416.

(54) Le, J.-B.; Cheng, J. Modeling electrified metal/water interfaces from ab initio molecular dynamics: Structure and Helmholtz capacitance. *Current Opinion in Electrochemistry* **2021**, *27*, 100693.

(55) Wakisaka, M.; Suzuki, H.; Mitsui, S.; Uchida, H.; Watanabe, M. Identification and Quantification of Oxygen Species Adsorbed on Pt(111) Single-Crystal and Polycrystalline Pt Electrodes by Photoelectron Spectroscopy. *Langmuir* **2009**, *25*, 1897–1900, PMID: 19152331.

(56) Wakisaka, M.; Udagawa, Y.; Suzuki, H.; Uchida, H.; Watanabe, M. Structural effects on the surface oxidation processes at Pt single-crystal electrodes studied by X-ray photoelectron spectroscopy. *Energy Environ. Sci.* **2011**, *4*, 1662–1666.

(57) Gómez-Marín, A. M.; Clavilier, J.; Feliu, J. M. Sequential Pt(111) oxide formation in perchloric acid: An electrochemical study of surface species inter-conversion. *Journal of Electroanalytical Chemistry* **2013**, *688*, 360–370, Special Issue in Honor of Professors Chuansin Cha and Zhaowu Tian.

(58) Chen, J.; Luo, S.; Liu, Y.; Chen, S. Theoretical Analysis of Electrochemical Formation and Phase Transition of Oxygenated Adsorbates on Pt(111). *ACS Applied Materials & Interfaces* **2016**, *8*, 20448–20458, PMID: 27377100.

(59) Huang, J.; Malek, A.; Zhang, J.; Eikerling, M. H. Non-monotonic Surface Charging Behavior of Platinum: A Paradigm Change. *The Journal of Physical Chemistry C* **2016**, *120*, 13587–13595.

(60) Jacob, T.; Goddard, W. A. Agostic Interactions and Dissociation in the First Layer of Water on Pt(111). *Journal of the American Chemical Society* **2004**, *126*, 9360–9368, PMID: 15281827.

(61) Site, L. D.; Ghiringhelli, L. M.; Andreussi, O.; Donadio, D.; Parrinello, M. The interplay between surface–water and hydrogen bonding in a water adlayer on Pt(111) and Ag(111). *Journal of Physics: Condensed Matter* **2007**, *19*, 242101.

(62) Ikeshoji, T.; Otani, M.; Hamada, I.; Sugino, O.; Morikawa, Y.; Okamoto, Y.; Qian, Y.; Yagi, I. The charged interface between Pt and water: First principles molecular dynamics simulations. *AIP Advances* **2012**, *2*, 032182.

(63) Zeng, Z.; Greeley, J. Characterization of oxygenated species at water/Pt(111) interfaces from DFT energetics and XPS simulations. *Nano Energy* **2016**, *29*, 369–377, Electrocatalysis.

(64) Franck, E. U. J. D. Cox, D. D. Wagman, V. A. Medvedev: CODATA — Key Values for Thermodynamics, aus der Reihe: CODATA, Series on Thermodynamic Properties. Hemisphere Publishing Corporation, New York, Washington, Philadelphia, London 1989. 271 Seiten, Preis: £ 28.00. *Berichte der Bunsengesellschaft für physikalische Chemie* **1990**, *94*, 93–93.

(65) Limmer, D. T.; Willard, A. P.; Madden, P.; Chandler, D. Hydration of metal sur-

faces can be dynamically heterogeneous and hydrophobic. *Proceedings of the National Academy of Sciences* **2013**, *110*, 4200–4205.

(66) Pajkossy, T.; Kolb, D. Double layer capacitance of Pt(111) single crystal electrodes. *Electrochimica Acta* **2001**, *46*, 3063–3071.